Title

Two surfaces of a conserved interdomain linker differentially affect output from the RST sensing module of the Bacillus subtilis stressosome.

Journal

Journal of bacteriology, 194(15)

ISSN

0021-9193

Authors

Gaidenko, Tatiana A
Bie, Xiaomei
Baldwin, Enoch P
et al.

Publication Date

2012-08-01

DOI

10.1128/jb.00583-12

Peer reviewed

Journal of Bacteriology

Two Surfaces of a Conserved Interdomain Linker Differentially Affect Output from the RST Sensing Module of the Bacillus subtilis Stressosome

Tatiana A. Gaidenko, Xiaomei Bie, Enoch P. Baldwin and Chester W. Price

J. Bacteriol. **2012, 194(15):3913. DOI: 10.1128/JB.00583-12. Published Ahead of Print 18 May 2012.**

JB
Journals.ASM.org

Two Surfaces of a Conserved Interdomain Linker Differentially Affect Output from the RST Sensing Module of the *Bacillus subtilis* Stressosome

Tatiana A. Gaidenko,[a] Xiaomei Bie,[a]* Enoch P. Baldwin,[b] and Chester W. Price[a]

Departments of Microbiology[a] and of Molecular and Cellular Biology,[b] University of California, Davis, California, USA

The stressosome is a 1.8-MDa cytoplasmic complex that conveys environmental signals to the σ^B stress factor of *Bacillus subtilis*. A functionally irreducible complex contains multiple copies of three proteins: the RsbRA coantagonist, RsbS antagonist, and RsbT serine-threonine kinase. Homologues of these proteins are coencoded in different genome contexts in diverse bacteria, forming a versatile sensing and transmission module called RST after its common constituents. However, the signaling pathway within the stressosome itself is not well defined. The N-terminal, nonheme globin domains of RsbRA project from the stressosome and are presumed to channel sensory input to the C-terminal STAS domains that form the complex core. A conserved, 13-residue α-helical linker connects these domains. We probed the *in vivo* role of the linker using alanine scanning mutagenesis, assaying stressosome output in *B. subtilis* via a σ^B-dependent reporter fusion. Substitutions at four conserved residues increased output 4- to 30-fold in unstressed cells, whereas substitutions at four nonconserved residues significantly decreased output. The periodicity of these effects supports a model in which RsbRA functions as a dimer *in vivo*, with the linkers forming parallel paired helices via a conserved interface. The periodicity further suggests that the opposite, nonconserved faces make additional contacts important for efficient stressosome operation. These results establish that the linker influences stressosome output under steady-state conditions. However, the stress response phenotypes of representative linker substitutions provide less support for the notion that the N-terminal globin domain senses acute environmental challenge and transmits this information via the linker helix.

Input (or sensory) domains of bacterial signaling proteins are often joined to output domains by amphipathic α-helices or coiled coils (2, 32, 36). Analysis of such helices should reveal common themes as well as differences regarding interdomain signal transmission. Here we report genetic analysis of a conserved, 13-residue linker that connects the presumed input and output domains in a widely distributed cytoplasmic signaling module, called RST after its three principal protein components (35). The RST module is encoded by diverse bacterial genomes, in contexts that suggest its sensory input can be adapted to control different signaling pathways.

The composition, physical arrangement, and physiological role of the RST module have been most intensively studied in the model Gram-positive bacterium *Bacillus subtilis*, where it regulates activation of the general stress factor σ^B in response to a variety of environmental signals, including acid, alcohol, heat, or salt stress (18, 37). *B. subtilis* RST components were found to form the stressosome (9, 11, 24, 29), a large cytoplasmic complex that consists of multiple copies of the RsbT serine-threonine kinase, the RsbS antagonist protein, and one or more members of the RsbR coantagonist family (where Rsb indicates regulator of sigma-B). *In vivo*, each stressosome appears to contain a mixture of the paralogous and partly redundant RsbRA, -RB, -RC, and -RD coantagonists (11, 24). Each of these coantagonists has an N-terminal, nonheme globin domain, a 13-residue interdomain linker, and a C-terminal STAS (sulfate transporter/anti-sigma factor antagonist) domain, whereas the smaller RsbS antagonist comprises only a STAS domain (29, 34).

Genetic and biochemical studies have shown that RsbRA, RsbS, and RsbT form a minimal functional stressosome (9, 24). Cryo-electron microscopy images of complexes assembled from purified components suggest an essentially icosahedral structure comprising the STAS domains of 20 RsbRA dimers and 20 RsbS monomers, which directly bind 20 RsbT kinase monomers to the outer surface of the icosahedron (29). The N-terminal, nonheme globin domains of the RsbRA dimers project outward from the core structure and are the presumed route of signal entry into the complex.

According to the model shown in Fig. 1, in unstressed cells the complex sequesters the RsbT switch protein/kinase and prevents it from binding its regulatory target, the RsbU environmental phosphatase. During the stress response, RsbT phosphorylates the RsbS antagonist on a conserved serine residue; this modification is associated with the release of RsbT from the complex and its subsequent activation of RsbU by direct protein-protein interaction. This basic model is well supported by genetic and biochemical analysis (9, 10, 12, 23, 43). However, the molecular events that promote RsbT release are not well understood. It has been proposed that stress signals elicit a conformational change in the N-terminal input domains of the RsbR coantagonists (29, 34). This change would then be communicated via the central helical link-

Received 6 April 2012 **Accepted** 10 May 2012
Published ahead of print 18 May 2012
Address correspondence to Chester W. Price, cwprice@ucdavis.edu.
* Present address: Xiaomei Bie, Department of Bioengineering, Nanjing Agricultural University, Nanjing, People's Republic of China.
Supplemental material for this article may be found at http://jb.asm.org/.

doi:10.1128/JB.00583-12

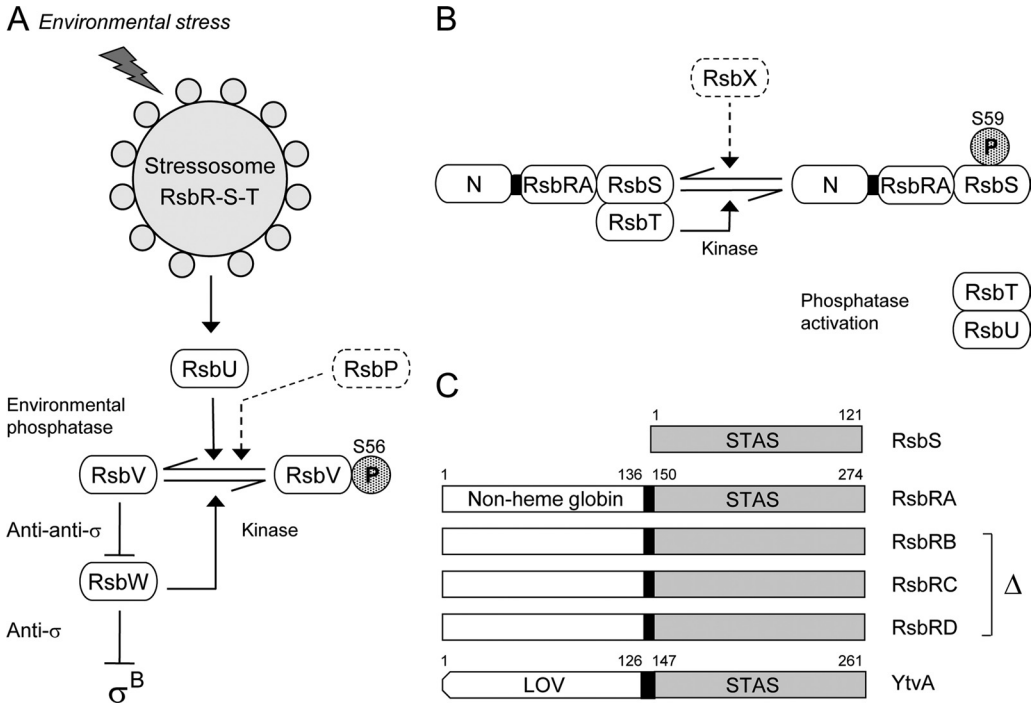

FIG 1 σ^B Regulatory network. (A) Model of signaling pathways that converge on the RsbV anti-anti-σ and RsbW anti-σ, which directly regulate σ^B activity. The stressosome controls activation of the RsbU environmental phosphatase in response to diverse signals. The separate RsbP energy phosphatase is not the focus here and is represented only in a dotted outline. Activated RsbU removes the phosphate (stippled P) from RsbV-P, the form found in unstressed cells. RsbV binds RsbW, forcing σ^B release. Arrowheads indicate activation of protein targets or enzymatic reactions; T-headed lines indicate inhibition. (B) Model of stressosome control of RsbU phosphatase activity. The stressosome comprises the partially redundant RsbRA, -RB, -RC, and -RD coantagonists (represented here as RsbRA, with its N-terminal, nonheme globin domain labeled N) and the RsbS antagonist, which together bind the RsbT kinase. During the stress response, RsbT phosphorylates its RsbS antagonist on S59; RsbT is released to bind and activate RsbU. The RsbX feedback phosphatase (dotted outline) dephosphorylates RsbS-P. (C) The RsbS antagonist has a single STAS domain (residues 1 to 121), whereas the RsbRA coantagonist has a nonheme globin domain (1 to 136) and a STAS domain (150 to 274) joined by the 13-residue helical linker analyzed here (black rectangle). RsbRB, -RC, and -RD coantagonists are structurally similar to RsbRA; these three paralogs were removed from most strains in the study. YtvA is an RsbR family member that positively controls stressosome output in response to blue light, sensed by its LOV domain (residues 1 to 126) and transmitted to STAS (147 to 261) by a 20-residue helical linker (black rectangle).

ers to the C-terminal STAS domains in the complex core and, presumably, to the adjacent STAS domain of the RsbS antagonist as well. A shift in core structure is thought to promote both activation of the RsbT kinase and its release from the complex.

This route of signal transmission within RsbRA is plausible, but there is no experimental evidence to support it. Although single substitutions within the N-terminal, nonheme globin domain were found to increase system output in unstressed cells, they had no effect on the magnitude of subsequent stress signaling (16). These results indicate that the N-terminal domain influences stressosome function but offer no direct support for the hypothesis that it is a stress sensor. Moreover, little is presently known regarding the function of the 13-residue linker that connects the N-terminal globin to the C-terminal STAS domain (29). Here we use alanine scanning mutagenesis to probe the *in vivo* operation of this linker, finding that substitutions at different positions had distinct effects on system output in unstressed cells. The periodicity of these effects supports a model in which two linkers associate as parallel paired helices within an RsbRA dimer, with the inside and outside surfaces of the pair making different protein contacts *in vivo*.

MATERIALS AND METHODS

Bacterial strains and genetic methods. Standard recombinant methods (40) and natural transformations (13) were used to construct the *B. subtilis* strains shown in Table S1 in the supplemental material. The plasmids employed in these constructions are listed in Table S2. A QuikChange Lightning kit (Stratagene, La Jolla, CA) was used to introduce missense substitutions into the linker region of the *rsbRA* gene encoded on integrative plasmid pTG5923 (16); substitution was confirmed by sequencing the entire coding region of each construction. These missense alleles were exchanged for wild-type *rsbRA* on the chromosome using the I-SceI-mediated method of Janes and Stibitz (20) as described previously (16). The constructed strains also carried a single-copy transcriptional fusion between the *ctc* promoter and a *lacZ* reporter to provide an indirect measure of σ^B activity (8).

β-Galactosidase accumulation assay and Western blots. Assays were conducted as described previously (16). Briefly, shake cultures were grown at 37°C in buffered Luria broth medium lacking salt (7), with moderate white-light illumination (3 to 4 μmol m^{-2} s^{-1}). This illumination saturated the blue-light-sensing YtvA positive regulator (5), an RsbR family member and stressosome constituent (17), ensuring that fluctuations in light intensity did not affect assay results. Unstressed samples were taken during early exponential growth up to a cell density of 20 absorbance units (Klett-Summerson colorimeter equipped with a number 66 transmission filter), at which point ethanol or NaCl stress was imposed at a final concentration of 4% (vol/vol) or 0.3 M, respectively. Samples were treated essentially according to the method of Miller (30); β-galactosidase activity was defined as $\Delta A_{420} \times 1{,}000$ min^{-1} mg^{-1} of protein (16). Basal activity was the value measured in unstressed cells at 20 absorbance units; stress activation was the difference between this basal value and the maximum activity realized after stressor addition.

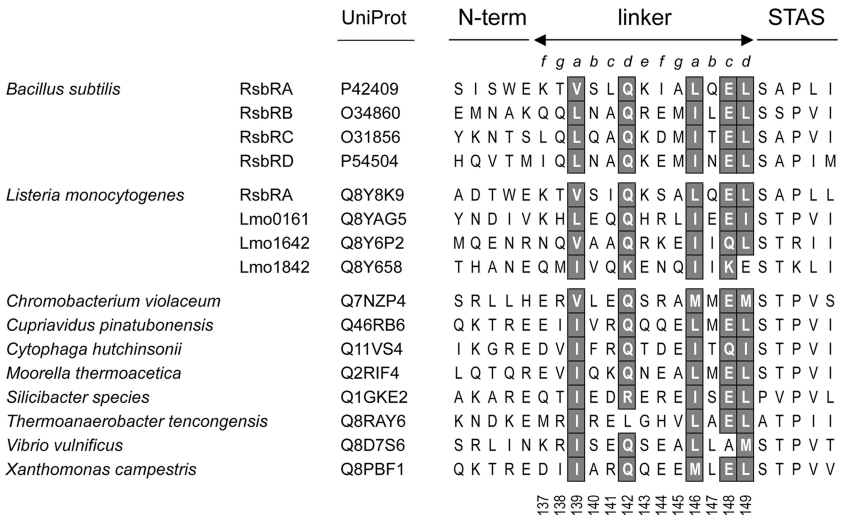

FIG 2 Conserved residues in diverse RsbR linkers. ClustalW alignment of the linker regions of RsbR paralogs from *B. subtilis* and *L. monocytogenes* plus the eight most diverse orthologs from Fig. S1 in the supplemental material, with the conserved positions shaded. Organism, paralog designation, and UniProt identifier indicate linker origin; lines and letters above alignment denote N-terminal and C-terminal domain boundaries and residue position within presumed heptad repeats; vertical numbers below the alignment are *B. subtilis* RsbRA residue numbers.

Western blotting, using mouse monoclonal anti-RsbRA antibody provided by William Haldenwang (14), was done as described previously (24). Forty micrograms of protein from wild and mutant cell extracts were separated by SDS-PAGE and transferred to polyvinylidene difluoride membranes (Bio-Rad Laboratories, Hercules, CA). Primary and secondary antibody binding was detected using the ECL Plus kit (Amersham Pharmacia Biotech, Piscataway NJ).

Bioinformatic methods. A database of RsbRA homologues was developed using the NCBI BLAST algorithm (1) at default settings. Full-length *B. subtilis* RsbRA (residues 1 to 274) was queried against the nonredundant database (1 March 2009 version). From the resulting hits, we selected those whose structural genes were encoded in an RST module (38). The list was further reduced by randomly choosing one representative per bacterial or archaeal genus, resulting in the 29 sequences shown in Fig. S1 in the supplemental material. These homologues all had N-terminal domains with a globin fold; some had sequences suggestive of heme binding but most appeared to be nonheme globins, like *B. subtilis* RsbRA. For the alignment shown in Fig. 2, we created a 16-member data set by combining the eight most diverse linker sequences from Fig. S1 (HHfilter utility from the MPI Bioinformatics Toolkit, http://toolkit.tuebingen.mpg.de/hhfilter) with those of the eight RsbR coantagonist paralogs encoded by the *B. subtilis* and *Listeria monocytogenes* genomes (35). Multiple alignment was done using ClustalW with default settings and the BLOSUM 62 matrix (42).

Computational modeling. Superpositions and structural analyses were carried out with EDPDB (44) and visualized and manipulated with the O crystallographic program (21). The 13-residue linker region of *B. subtilis* RsbRA was modeled as a coiled-coil extension of the globin domain crystal structure (34) (PDB accession number 2BNL). We exploited the similar dispositions of the RsbRA dimer C-terminal and the basic regions of the GCN4/DNA complex model (15) (PDB accession number 1YSA). Initial structural alignments were established by manually docking the 1YSA CD dimer to the 2BNL AB dimer, followed by least-squares superposition of 1YSA residues C254 to C261 and D254 to D261 on 2BNL residues A129 to A136 and B129 to B136 (main-chain root mean square deviation [RMSD] = 1.27 Å). This transformation was used to position the GCN4 coiled-coil region as a helical extension of 2BNL. The equivalent 1YSA residues 262 to 274 were converted to RsbRA linker residues 137 to 149, and the least-hindered side chain rotamers were chosen without further optimization.

Although the continuous helical model is the most parsimonious, other helical registers were investigated by modeling the 13 linker residues in 7 registers (±3 residues from the continuous model, the "0" register). In the 0-register model, three of the five large, nonpolar residues pair at the interface (V139, L146, and L149, along with A145) while two others cluster on the outer face of each helix (L141 and I144). Besides the 0-register, only the −2 register significantly buries some nonpolar residues (L141 and I144) while exposing others (V139, L146, and L149). In all other registers, four or five nonpolar residues were solvent exposed. The 0-register arrangement is in good agreement with the recently determined structure of the *Moorella thermoacetica* RsbR homolog (39) (PDB accession number 3ZTA), which contains the helical extension (main-chain RMSD of 1.10 Å for RsbRA linker dimer model residues 137 to 149 superimposed on the 3ZTA crystallographic dimer residues 132 to 144).

RESULTS

Linker sequences are conserved at specific positions. We first compared the sequence of the 13-residue *B. subtilis* RsbRA linker with orthologs found in diverse RST modules as well as with paralogs encoded separately from these modules, such as the coantagonist paralogs of *B. subtilis* and *L. monocytogenes* (35). The N-terminal domains of these proteins all exhibit a globin fold but otherwise share little sequence identity. A multiple alignment of 16 representative linker sequences is shown in Fig. 2. The N-terminal boundary of the linker is set by E136, which marks the last residue of the available nonheme globin structure of *B. subtilis* RsbRA (34). This glutamate is conserved among the RsbRA orthologs in the figure but less so among the paralogs. The C-terminal boundary is set by the ELSAP motif that forms the junction between the linker and the STAS domain, with SAP (or STP) marking the beginning of STAS (3).

The constancy of the multiple alignment argues for a conserved linker structure, and its heptad periodicity resembles that of α-helical coiled coils. Coiled coils result from the packing of two or more α-helices that manifest a repeat pattern *a-b-c-d-e-f-g*, in which positions *a* and *d* are usually occupied by hydrophobic residues (27). Here the *B. subtilis* RsbRA linker begins with a lysine (K137) at a presumptive *f* position. A conserved hydrophobic res-

idue (V139) occupies the first *a* position, whereas an atypical but highly conserved glutamine (Q142) is found at the first *d* position. In contrast, conserved hydrophobic residues (L146 and L149) lie at both the second *a* and *d* positions. The *c* position (E148) of this second, incomplete heptad is also highly conserved and marks the beginning of the ELSAP motif that joins the linker and STAS domain. Secondary structure predictions (not shown) suggest that each linker forms an extension of the final α-helix of the N-terminal globin fold, termed the H helix in the *B. subtilis* RsbRA structure (34). Thus, motion within the N-terminal domain could be transmitted to the STAS domain within the stressosome core by means of this extended helix.

Phenotypes conferred by linker substitutions suggest two separate interacting surfaces. We performed alanine scanning mutagenesis on 12 of the 13 *B. subtilis* residues, leaving A145 unexamined. We made additional disruptive substitutions at V139, L146, E148, and L149, which occupy positions conserved in the multiple alignment, and also at K143, whose charge is conserved among all four *B. subtilis* RsbR paralogs. These disruptive substitutions involved either the replacement of a hydrophobic residue with an arginine (e.g., V139R) or a reversal of charge (e.g., K143E). A two-step procedure was used to exchange the mutant *rsbRA* alleles encoding each substitution for the wild-type allele on the *B. subtilis* chromosome. Because the presence of the paralogous RsbRB, -RC, and -RD coantagonists can mask the phenotypes of *rsbRA* mutations (16), we assayed the effect of each substitution on expression of a σ^B-dependent reporter fusion in a strain bearing null alleles of *rsbRB*, *rsbRC*, and *rsbRD*.

In general, phenotypes elicited by the alanine substitutions were qualitatively similar to those of the more disruptive changes (Fig. 3). Alanine substitution at the conserved Q142, L146, E148, and L149 positions increased σ^B activity 4- to 30-fold in unstressed cells. However, alanine substitution at the conserved V139 only slightly increased σ^B activity, while substitution at the more narrowly conserved K143 only slightly decreased it (Fig. 3A). These latter phenotypes became markedly more pronounced in strains bearing the disruptive V139R and K143E substitutions, and they altered σ^B activity the same direction as the corresponding alanine changes (Fig. 3B). An exception to this qualitative similarity occurred with the L149R substitution, which reversed the elevated phenotype of its L149A counterpart by decreasing σ^B activity from control levels. To resolve this difference, we made an additional disruptive substitution, L149D, and found it increased σ^B activity much like L149A. These results indicate that substitutions at L149 can have a range of phenotypes. Nonetheless, alanine substitutions at any of the five conserved residues–V139, Q142, L146, E148, and L149–have the common property of increased system output in unstressed cells.

Notably, alanine substitutions at five of the nonconserved positions also had significant effects. As was the case for the conserved positions, a T138A substitution increased σ^B activity in unstressed cells by more than 20-fold (Fig. 3A). In contrast, the S140A, L141A, and Q147A substitutions decreased σ^B activity 6- to 9-fold, whereas I144A decreased it about 2-fold. None of these four restricting alanine substitutions would be expected to disrupt or destabilize the helical structure.

With the exception of E148, the conserved positions at which alanine substitution significantly increased stressosome output lie on one face of a helical wheel representation, and T138 with its similar phenotype is on this same face (Fig. 3C).

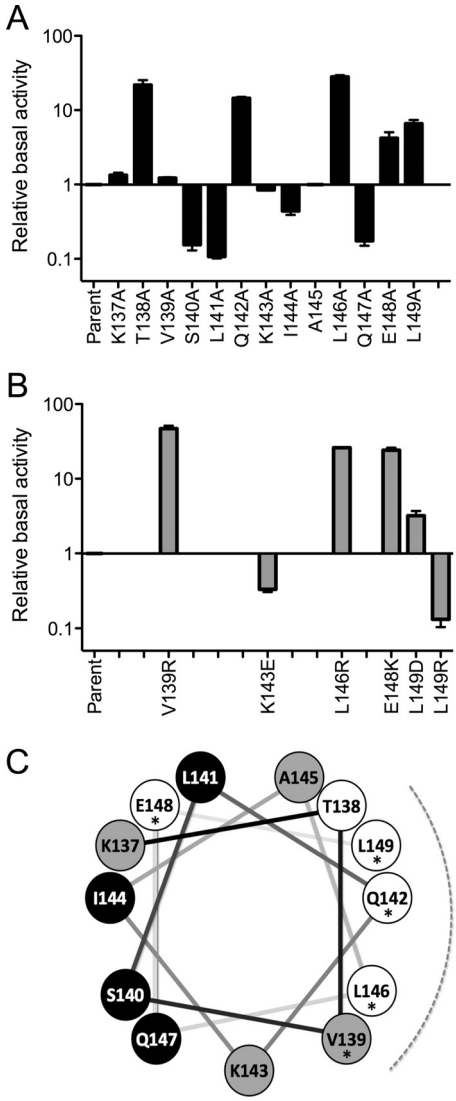

FIG 3 Effects of linker substitutions on σ^B activity in unstressed cells. (A) Relative activity elicited by alanine substitutions, with the parent strain taken as 1 (PB1078, encoding RsbRA as the only coantagonist). β-Galactosidase accumulation from a *ctc-lacZ* fusion was assayed in logarithmically growing cells; error bars indicate standard errors of the means (SEM) from at least two independent experiments. (B) Relative activity of more disruptive substitutions at conserved positions, with the parent strain taken as 1. (C) Helical wheel representation of the RsbRA linker, with the conserved positions indicated by asterisks, the conserved face by the dotted curve, and the effect of alanine substitution by fill color. Substitutions on the conserved face enhanced output (T138, Q142, L146, L149; white circles), whereas those on the opposite face diminished it (S140, L141, I144, Q147; black circles). Alanine substitutions at the N terminus of the linker (K137) or between the two faces (V139 and K143) had little effect (gray circles). Alanine substitution at E148 was not in accord with this pattern: output was enhanced, but E148 lies on the face opposite the other conserved residues with a similar phenotype.

In contrast, all of the nonconserved positions at which substitution decreased output lie on the opposite face. The two positions at which phenotypes were made plain only with more disruptive substitutions, V139 and K143, lie between these faces. Based on these striking phenotypic patterns, we infer that the linker helix has two discrete surfaces which interact with different partners.

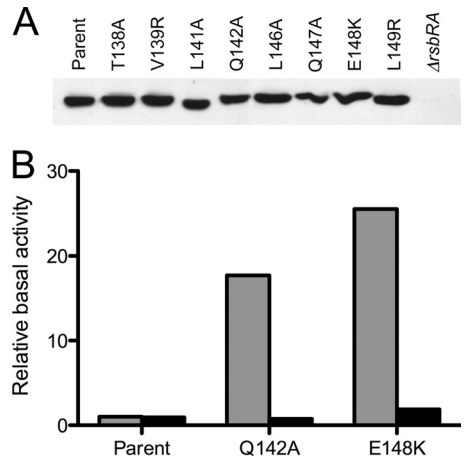

FIG 4 Representative substitutions did not affect *in vivo* levels of RsbRA or its ability to form stressosomes. (A) Relative steady-state levels of wild and mutant RsbRA proteins estimated by Western blotting. Extracts of cells bearing designated substitutions were separated by PAGE and probed with anti-RsbRA antibody. (B) Genetic suppression analysis indicates that RsbRA proteins with Q142A and E148K substitutions form functional stressosomes. Relative activities in strains with each designated substitution are indicated by gray bars; activities with the same substitution coupled with the S59A substitution in RsbS are indicated by black bars. Assays were performed on unstressed cells as described in the Fig. 3 legend; activities are expressed with the parent strain taken as 1 (PB1078, encoding RsbRA as the only coantagonist).

Suppression analysis indicates that mutant RsbRA proteins form functional stressosomes. The RsbR coantagonists have a negative regulatory role in *B. subtilis*, and at least one of the four is needed to join with the RsbS antagonist to bind RsbT and keep system output low in unstressed cells (9, 11, 24). By design, our assay strain encoded only the RsbRA paralog. Therefore, substitutions at conserved linker positions might elevate σ^B activity due to a partial loss of the ability of RsbRA to assemble with RsbS and form functional stressosomes. We used two different approaches to evaluate the properties of mutant RsbRA proteins *in vivo*.

First, Western blotting estimated RsbRA levels in six strains bearing substitutions that strongly increased system output, as well as for two strains with substitutions that significantly decreased it. As shown in Fig. 4A, none of the mutant strains had a steady-state RsbRA level that was noticeably different from the wild-type control. Therefore, elevated σ^B activity in the six enhancing mutants was not simply due to a decreased amount of RsbRA.

Second, genetic suppression tested the functionality of stressosomes formed with mutant RsbRA proteins. The RsbS antagonist requires an RsbR coantagonist to effectively bind RsbT *in vitro* and prevent high constitutive signaling *in vivo* (9, 24). Following an environmental stress, the RsbT kinase contributes to the efficiency of its own release from the stressosome by phosphorylating RsbS on serine 59 (9, 25, 28, 43). A phosphorylation-deficient S59A substitution therefore greatly dampens σ^B activation, but it cannot compensate for the absence of RsbR coantagonist function in sequestering RsbT (23, 24). Beginning with a genetic background in which RsbRA was the only coantagonist present, we combined the allele encoding RsbS-S59A with either Q142A or E148K, representative substitutions that strongly increased system output in unstressed cells. As shown in Fig. 4B, with both RsbRA mutants, the RsbS-S59A allele restored σ^B activity to the basal level of the parent strain.

This suppression of the mutant phenotype indicates that the tested RsbRA proteins can form stressosomes capable of sequestering RsbT. This result also suggests that the elevated basal level caused by the Q142A or E148K substitution in part reflects abnormally high S59 phosphorylation in unstressed cells. A further indication of the functionality of the mutant stressosomes is their ability to support an environmental stress response, which is described in the next section.

Effect of linker substitutions on stress response. The previous assays addressed the effect of linker substitutions on the steady-state (or basal) output of the complex in unstressed cells. To assess their impact on stress signaling, we determined the phenotypes of representative substitutions in logarithmically growing cells exposed to moderate or mild environmental stresses (4% ethanol or 0.3 M NaCl, respectively).

The Q142A, L146A, and E148K substitutions, which enhanced steady-state output 14- to 30-fold in unstressed cells, had no significant effect on the magnitude of subsequent stress signaling (Fig. 5). These phenotypes resemble those of the previously characterized K82A and K93A substitutions within the N-terminal, nonheme globin domain of RsbRA: elevated basal levels but no effect on stress response (16).

The Q147A and L141A substitutions, which restricted output 6- or 9-fold in unstressed cells, also had no significant effect on ethanol stress signaling (Fig. 5). However, these restricting substitutions did reduce the NaCl response by 2- or 4-fold, respectively. Such a diminished response to mild stress probably reflects the lower basal level of σ^B activity in these strains, which would slow the autocatalytic induction of σ^B and result in decreased stress sensitivity (19). This consideration cannot fully explain the phenotype of the L149R substitution, which restricted output by a comparable amount in unstressed cells (7-fold) but diminished response to NaCl stress by more than 50-fold (Fig. 5). These restrictive substitutions collectively represent two new classes of *rsbRA* mutant: significantly reduced basal output with either a modest (Q147A or L141A) or strong (L149R) impact on NaCl response. Notably, only the disruptive L149R substitution had this strong phenotype. Its L149A cousin resembled the Q142A, L146A, and E148K enhancing substitutions, with an elevated basal level (Fig. 3) but no significant effect on stress response (data not shown).

Phenotypes of enhancing substitutions are masked in the presence of other RsbR paralogs. In the standard assay strain in which the mutant *rsbRA* allele encoded the only functional coantagonist, the Q142A and E148K substitutions greatly increased basal output compared to the wild-type allele (Fig. 3). However, these strong enhancing phenotypes were completely masked in a strain that also encoded the other three members of the coantagonist family, RsbRB, -RC, and -RD (see Fig. S2 in the supplemental material). Thus, the stressosome complement of the cell must be formed solely from the mutant coantagonist for the phenotype to be revealed.

DISCUSSION

RsbRA and its coantagonist paralogs are thought to comprise the initial sensory and transmission components of a widespread bacterial signaling module, which in *B. subtilis* forms the σ^B-activating stressosome (35). Here we used alanine scanning and other

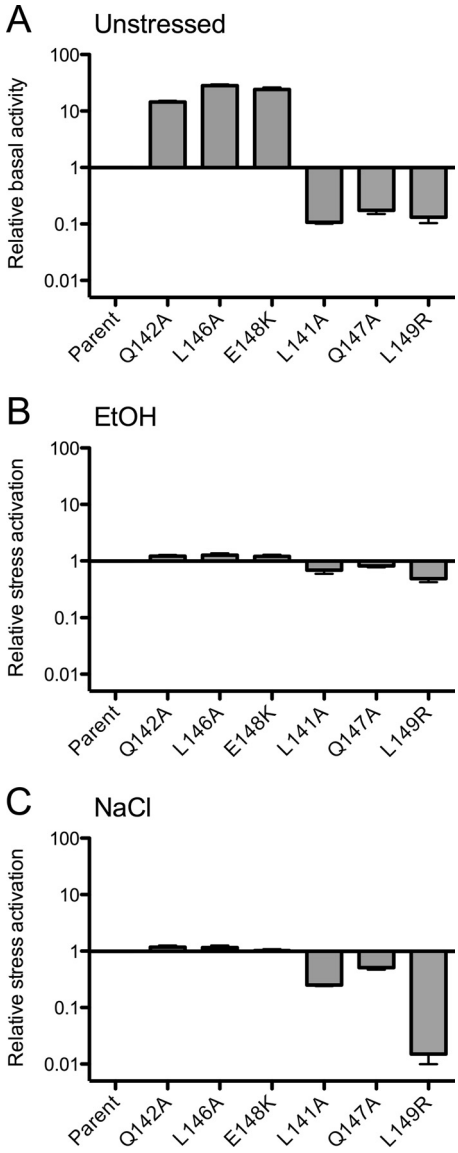

FIG 5 Effect of representative linker substitutions on stress activation. (A) Data showing relative basal activity in unstressed cells is from Fig. 3, with activity of the parent strain (PB1078, encoding RsbRA as the only coantagonist) taken as 1. Relative activation following 4% ethanol (B) or 0.3 M NaCl (C) stress, with activation of the parent strain taken as 1. Error bars indicate SEM from at least two independent experiments.

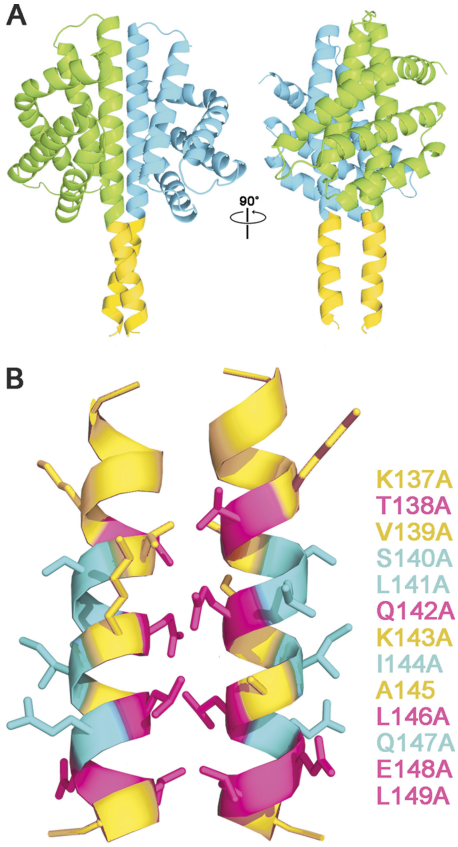

FIG 6 Computational model of paired RsbRA linker helices, derived by extending the H helices of the nonheme globin crystal structure (PDB code 2BNL, chains A and B, cyan and green ribbons) to include the linker helices (gold ribbons, RsbRA residues 137 to 150; see Materials and Methods). (A) Two views of the nonheme globin dimer showing crossover of the linker helices at Q142 (left) and a 90° rotated view looking into the putative interaction surfaces of the paired helices (right). (B) Details of the interaction surfaces, indicating the effects of alanine substitution at positions 137 to 149: substitutions that enhance steady-state output of the stressosome (magenta), those that diminish output (cyan), and those with no significant effect (gold). This correspondence of helical periodicity with mutational phenotype is consistent with the notion that each linker helix interacts with two different binding partners: its counterpart helix via the highly conserved interface residues and an unknown partner via the nonconserved residues on the opposite face.

missense substitutions to probe the role of a conserved 13-residue linker that connects the presumed input and output domains of RsbRA (29). Our results firmly tie the linker to the control of output levels in unstressed cells but offer less support for a role in conveying signals of acute environmental stress.

In general, the phenotypes elicited by the alanine substitutions manifested a striking periodicity: those on the conserved face of the helix led to elevated steady-state output from the stressosome, whereas those on the opposite, nonconserved face led to decreased output. We interpret these results to indicate that the two helical faces interact with different partners *in vivo*. A differential interaction can be most simply explained by the computational model shown in Fig. 6. In this model, the H helices of the globin dimer structure of Murray et al. (34) have been extended to include the adjacent 13-residue linkers, which then form parallel paired helices via their conserved interfacial residues. In this configuration, the nonconserved residues on the opposite face of the linker are free to contact a different binding partner.

The model is supported by the similar phenotypes of both N-terminal and linker substitutions that are predicted to affect RsbRA dimerization. The isolated N-terminal, nonheme globin domains of RsbRA form homodimers both in solution and during crystallization (34). Based on the crystal structure, the K82A and K93A substitutions within this domain would be expected to adversely affect homodimer formation, and both substitutions were previously found to share a distinctive phenotype: elevated basal output in unstressed cells but no significant effect on subsequent stress signaling (16). From the computation model shown in Fig. 6, we predict that the Q142A and L146A substitutions tested here would adversely affect interaction of the paired linker helices,

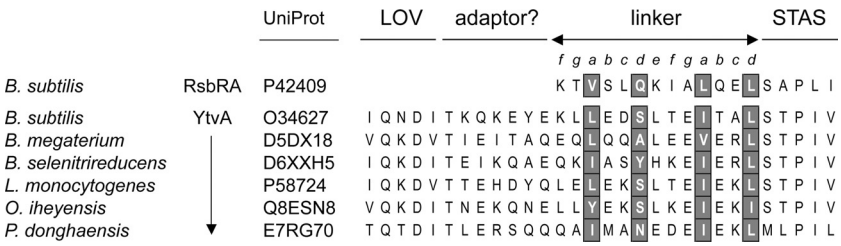

FIG 7 Comparison of the RsbRA linker with Jα linkers from diverse YtvA orthologs. YtvA is an RsbRA-like stressosome component that senses blue light via its N-terminal LOV domain, communicating this to its C-terminal STAS domain by means of a 20-residue Jα helix (see Discussion). The C-terminal 13 residues of representative Jα linkers are aligned with the *B. subtilis* RsbRA linker, with the conserved positions shaded. Lines and letters above the alignment show N- and C-terminal domain boundaries and the residue position within the presumed heptad repeats.

and these substitutions had the same characteristic phenotypes as the K82A and K93A globin substitutions. Our genetic results support the notion that the N-terminal region of RsbRA normally functions as a dimer *in vivo* and further suggest that the dimerization interface encompasses both the nonheme globin domain and the paired linker helices that are extensions of this domain.

The phenotypes caused by alanine substitution at the nonconserved S140, L141, I144, and Q147 residues were unexpected: decreased basal output in unstressed cells, coupled with a modest decrease in stress signaling for the representatives tested. Because none of these substitutions would alter linker helicity, we conclude that the absent side chains provide inter- or intramolecular contacts that contribute to normal stressosome operation. Due to steric and topological considerations, the outer faces of the paired linker helices are unlikely to directly contact the N-terminal, nonheme globin domain. Possible interacting partners therefore include an unknown small molecule or protein, the RsbT kinase, or the nearby STAS domain of RsbRA itself. In the latter case, the nonconserved face of the helix may promote the efficient coupling of the N- and C-terminal domains.

The phenotypes of substitutions at the conserved E148 and L149 residues are at variance with the simplest view of two interacting faces. However, these exceptional phenotypes could signal a different role of these particular residues in coupling the linker and STAS domain. According to the computational model, E148 points away from the helical interface, but E148A and E148K elicited the same distinctive phenotype as substitutions at the Q142 and L146 interface residues: elevated steady-state output with no effect on stress response. This distinguishes E148 from the restricting S140, L141, L144, and Q147 substitutions on the same helical face, suggesting that the E148 side chain contacts a different partner or a different part of the STAS domain. On the other hand, the characteristic elevated phenotype of L149A was consistent with an interface role, but the disruptive L149R phenotype had the opposite phenotype: diminished steady-state output and a severe effect on the response to NaCl stress. We speculate that the arginine side chain effectively jams the linker-STAS interface in a less-responsive conformation.

Because full-length RsbRA aggregates *in vitro*, as yet, there is no complete structure to corroborate these genetic inferences. However, studies of two related proteins are informative. The crystal structure of the N-terminal, nonheme globin domain of the RsbRA ortholog from the *Moorella thermoacetica* stressosome (PDB accession number 3ZTA) also includes the linker residues (39). This domain shares only 12% sequence identity with its *B. subtilis* counterpart but is structurally equivalent. Notably, its associated linkers form parallel helices at the dimerization interface, which is in good agreement with the computational model shown in Fig. 6 (see Materials and Methods). Other studies have focused on the RsbRA paralog YtvA. Like RsbRA, YtvA is associated with the *B. subtilis* stressosome but has no apparent coantagonist function, acting only as a positive signaling element in response to blue light (4, 6, 17). It has a domain organization similar to RsbRA and forms a head-to-head homodimer in solution (22). As shown in Fig. 1, instead of an N-terminal, nonheme globin, YtvA has a light-sensing LOV (light-oxygen-voltage) domain (26, 33) connected to a C-terminal STAS domain via a 20-residue Jα helix, the properties of which suggest formation of a parallel coiled coil in the YtvA homodimer (31). Structural studies indicate that light incidence brings about a small relative rotation of LOV monomers within a dimer crystal (33), and analysis of hybrid proteins suggests that Jα transfers this rotation to an output domain (31). Nuclear magnetic resonance studies of the full-length YtvA homodimer find that the C-terminal region of Jα is less flexible than the central part of the linker, supporting a role in coupling Jα to STAS (22).

The Jα helices of YtvA orthologs have little sequence similarity with the shorter RsbR linkers. However, as shown in Fig. 7, the C-terminal 13 residues of representative Jα helices share a heptad periodicity resembling that of the RsbR linkers, although in Jα a small residue (rather than a glutamine) usually occupies the *d* position of the first heptad. We speculate (i) that the seven N-terminal residues of Jα serve to adapt it to the LOV domain, (ii) that such an adaptor is unnecessary for the nonheme globin domain of RsbRA, and (iii) that the 13 C-terminal residues serve a similar role in Jα and the RsbR linker: transmitting information from the N-terminal domain to STAS.

The YtvA paralog provides a logical prototype of signaling from an N-terminal sensor domain to a C-terminal STAS output domain. However, the question of whether the nonheme globin domain of RsbRA is a sensor of acute environmental stress is unresolved. Characterization of two similar nonheme globin domains that modulate sporulation in *Bacillus anthracis* suggests that they are capable of sensing fatty acids and chloride via binding within a distinctive tunnel and chamber (41). The lack of these structural features seems to preclude the *B. subtilis* domain from sensing similar signals, and the cellular parameter to which it responds remains unknown. Furthermore, our genetic analyses of both the RsbRA N-terminal domain (16) and linker (this study) yielded results that are not in keeping with the usual N- to C-terminal route of information transfer within bacterial signaling proteins. Surprisingly, substitutions predicted to disrupt dimeriza-

tion of the N-terminal region increased stressosome output as much as 30-fold in unstressed cells but had no effect on the magnitude of ethanol or salt response.

At minimum, our results indicate that stressosome signaling has unusual features that remain to be explained. They also raise the possibility of an alternative hypothesis: the N-terminal sensory domains of RsbR family members primarily serve to adjust steady-state output of the stressosome. In the case of YtvA, this adjustment would be in response to blue light, whereas for RsbRA, it would be in response to a cytoplasmic parameter yet to be identified. In this view, the true sensor of acute ethanol or salt challenge lies downstream from the N-terminal, nonheme globin domain. This downstream sensor might comprise the arrangement of C-terminal STAS domains within the icosahedral core of the stressosome, in which stress-influenced shifts of conformational equilibria could directly affect RsbT release by increasing its dissociation rate. The two alternative models, N- or C-terminal domain as the environmental stress sensor, might be distinguished by substitutions in the RsbRA N-terminal region that specifically influence stress response while leaving steady-state output unchanged. The L149R substitution described here does affect stress signaling to a greater extent than steady state. However, due to its equivocal effects and position at the linker-STAS interface, the L149R phenotype is compatible with either model.

ACKNOWLEDGMENTS

We thank Lily Yang for her assistance in constructing the linker substitutions, William Haldenwang for providing the anti-RsbRA antibody, and Valley Stewart for helpful comments on the manuscript.

This research was supported by Public Health Service grant RO1 GM42077 from the National Institute of General Medical Sciences.

REFERENCES

1. **Altschul SF, et al.** 1997. Gapped BLAST and PSI-BLAST: a new generation of protein database search programs. Nucleic Acids Res. **25**:3389–3402.
2. **Anantharaman V, Balaji S, Aravind L.** 2006. The signaling helix: a common functional theme in diverse signaling proteins. Biol. Direct **1**:25.
3. **Aravind L, Koonin EV.** 2000. The STAS domain—a link between anion transporters and antisigma-factor antagonists. Curr. Biol. **10**:R53–R55.
4. **Avila-Pérez M, Hellingwerf KJ, Kort R.** 2006. Blue light activates the σ^B-dependent stress response of *Bacillus subtilis* via YtvA. J. Bacteriol. **188**:6411–6414.
5. **Avila-Pérez M, van der Steen JB, Kort R, Hellingwerf KJ.** 2010. Red light activates the σ^B-mediated general stress response of *Bacillus subtilis* via the energy branch of the upstream signaling cascade. J. Bacteriol. **192**:755–762.
6. **Avila-Pérez M, et al.** 2009. In vivo mutational analysis of YtvA from *Bacillus subtilis*: mechanism of light activation of the general stress response. J. Biol. Chem. **284**:24958–24964.
7. **Boylan SA, Redfield AR, Brody MS, Price CW.** 1993. Stress-induced activation of the σ^B transcription factor of *Bacillus subtilis*. J. Bacteriol. **175**:7931–7937.
8. **Boylan SA, Rutherford A, Thomas SM, Price CW.** 1992. Activation of *Bacillus subtilis* transcription factor σ^B by a regulatory pathway responsive to stationary-phase signals. J. Bacteriol. **174**:3695–3706.
9. **Chen CC, Lewis RJ, Harris R, Yudkin MD, Delumeau O.** 2003. A supramolecular complex in the environmental stress signalling pathway of *Bacillus subtilis*. Mol. Microbiol. **49**:1657–1669.
10. **Chen CC, Yudkin MD, Delumeau O.** 2004. Phosphorylation and RsbX-dependent dephosphorylation of RsbR in the RsbR-RsbS complex of *Bacillus subtilis*. J. Bacteriol. **186**:6830–6836.
11. **Delumeau O, Chen CC, Murray JW, Yudkin MD, Lewis RJ.** 2006. High-molecular-weight complexes of RsbR and paralogues in the environmental signaling pathway of *Bacillus subtilis*. J. Bacteriol. **188**:7885–7892.
12. **Delumeau O, et al.** 2004. Functional and structural characterization of RsbU, a stress signaling protein phosphatase 2C. J. Biol. Chem. **279**:40927–40937.
13. **Dubnau D, Davidoff-Abelson R.** 1971. Fate of transforming DNA following uptake by competent *Bacillus subtilis*. I. Formation and properties of the donor-recipient complex. J. Mol. Biol. **56**:209–221.
14. **Dufour A, Voelker U, Voelker A, Haldenwang WG.** 1996. Relative levels and fractionation properties of *Bacillus subtilis* σ^B and its regulators during balanced growth and stress. J. Bacteriol. **178**:3701–3709.
15. **Ellenberger TE, Brandl CJ, Struhl K, Harrison SC.** 1992. The GCN4 basic region leucine zipper binds DNA as a dimer of uninterrupted α helices: crystal structure of the protein-DNA complex. Cell **71**:1223–1237.
16. **Gaidenko TA, Bie X, Baldwin EP, Price CW.** 2011. Substitutions in the presumed sensing domain of the *Bacillus subtilis* stressosome affect its basal output but not response to environmental signals. J. Bacteriol. **193**:3588–3597.
17. **Gaidenko TA, Kim TJ, Weigel AL, Brody MS, Price CW.** 2006. The blue-light receptor YtvA acts in the environmental stress signaling pathway of *Bacillus subtilis*. J. Bacteriol. **188**:6387–6395.
18. **Hecker M, Pané-Farré J, Völker U.** 2007. SigB-dependent general stress response in *Bacillus subtilis* and related gram-positive bacteria. Annu. Rev. Microbiol. **61**:215–236.
19. **Igoshin OA, Brody MS, Price CW, Savageau MA.** 2007. Distinctive topologies of partner-switching signaling networks correlate with their physiological roles. J. Mol. Biol. **369**:1333–1352.
20. **Janes BK, Stibitz S.** 2006. Routine markerless gene replacement in *Bacillus anthracis*. Infect. Immun. **74**:1949–1953.
21. **Jones TA, Zou JY, Cowan SW, Kjeldgaard M.** 1991. Improved methods for building protein models in electron density maps and the location of errors in these models. Acta Crystallogr. A **47**:110–119.
22. **Jurk M, Dorn M, Schmieder P.** 2011. Blue flickers of hope: secondary structure, dynamics, and putative dimerization interface of the blue-light receptor YtvA from *Bacillus subtilis*. Biochemistry **50**:8163–8171.
23. **Kang CM, Brody MS, Akbar S, Yang X, Price CW.** 1996. Homologous pairs of regulatory proteins control activity of *Bacillus subtilis* transcription factor σ^B in response to environmental stress. J. Bacteriol. **178**:3846–3853.
24. **Kim TJ, Gaidenko TA, Price CW.** 2004. A multicomponent protein complex mediates environmental stress signaling in *Bacillus subtilis*. J. Mol. Biol. **341**:135–150.
25. **Kim TJ, Gaidenko TA, Price CW.** 2004. In vivo phosphorylation of partner switching regulators correlates with stress transmission in the environmental signaling pathway of *Bacillus subtilis*. J. Bacteriol. **186**:6124–6132.
26. **Losi A, Polverini E, Quest B, Gärtner W.** 2002. First evidence for phototropin-related blue-light receptors in prokaryotes. Biophys. J. **82**:2627–2634.
27. **Lupas AN, Gruber M.** 2005. The structure of α-helical coiled coils. Adv. Protein Chem. **70**:37–78.
28. **Macek B, et al.** 2007. The serine/threonine/tyrosine phosphoproteome of the model bacterium *Bacillus subtilis*. Mol. Cell. Proteomics **6**:697–707.
29. **Marles-Wright J, et al.** 2008. Molecular architecture of the "stressosome," a signal integration and transduction hub. Science **322**:92–96.
30. **Miller JH.** 1972. Experiments in molecular genetics. Cold Spring Harbor Laboratory, Cold Spring Harbor, NY.
31. **Möglich A, Ayers RA, Moffat K.** 2009. Design and signaling mechanism of light-regulated histidine kinases. J. Mol. Biol. **385**:1433–1444.
32. **Möglich A, Ayers RA, Moffat K.** 2009. Structure and signaling mechanism of Per-ARNT-Sim domains. Structure **17**:1282–1294.
33. **Möglich A, Moffat K.** 2007. Structural basis for light-dependent signaling in the dimeric LOV domain of the photosensor YtvA. J. Mol. Biol. **373**:112–126.
34. **Murray JW, Delumeau O, Lewis RJ.** 2005. Structure of a nonheme globin in environmental stress signaling. Proc. Natl. Acad. Sci. U. S. A. **102**:17320–17325.
35. **Pané-Farré J, Lewis RJ, Stülke J.** 2005. The RsbRST stress module in bacteria: a signalling system that may interact with different output modules. J. Mol. Microbiol. Biotechnol. **9**:65–76.
36. **Parkinson JS.** 2010. Signaling mechanisms of HAMP domains in chemoreceptors and sensor kinases. Annu. Rev. Microbiol. **64**:101–122.
37. **Price CW.** 2010. General stress response in *Bacillus subtilis* and related

Gram positive bacteria, p 301–318. *In* Storz G, Hengge R (ed), Bacterial stress responses, 2nd ed. ASM Press, Washington, DC.
38. **Pruitt KD, Tatusova T, Maglott DR.** 2007. NCBI reference sequences (RefSeq): a curated non-redundant sequence database of genomes, transcripts and proteins. Nucleic Acids Res. **35**:D61–D65.
39. **Quin MB, et al.** 2012. The bacterial stressosome: a modular system that has been adapted to control secondary messenger signaling. Structure **20**: 350–363.
40. **Sambrook J, Fritsch EF, Maniatis T.** 1989. Molecular cloning: a laboratory manual, 2nd ed. Cold Spring Harbor Laboratory, Cold Spring Harbor, NY.
41. **Stranzl GR, et al.** 2011. Structural insights into inhibition of *Bacillus anthracis* sporulation by a novel class of non-heme globin sensor domains. J. Biol. Chem. **286**:8448–8458.
42. **Thompson JD, Higgins DG, Gibson TJ.** 1994. CLUSTAL W: improving the sensitivity of progressive multiple sequence alignment through sequence weighting, position-specific gap penalties and weight matrix choice. Nucleic Acids Res. **22**:4673–4680.
43. **Yang X, Kang CM, Brody MS, Price CW.** 1996. Opposing pairs of serine protein kinases and phosphatases transmit signals of environmental stress to activate a bacterial transcription factor. Genes Dev. **10**:2265–2275.
44. **Zhang X-J, Matthews BW.** 1995. EDPDB: a multifunctional tool for protein structure analysis. J. Appl. Crystallogr. **28**:624–630.

Supplemental Material for Gaidenko *et al*.

Supplemental Tables S1, S2; Supplemental Figures S1, S2; Supplemental figure legends S1, S2.

Table S1. *Bacillus subtilis* strains

Strain	Genotype	Construction[1]
PB2	*trpC2*	168 Marburg strain
PB198	*amyE::ctc-lacZ trpC2*	(1)
PB1078	*rsbRBΔ2 rsbRCΔ1::ery rsbRDΔ2 amyE::ctc-lacZ trpC2*	(3)
PB1105	*rsbRA* K143E *rsbRBΔ2 rsbRDΔ2 rsbRCΔ1::ery amyE::ctc-lacZ trpC2*	pTG5973 → PB1078[2]
PB1107	*rsbRA* Q142A *rsbRBΔ2 rsbRDΔ2 rsbRCΔ1::ery amyE::ctc-lacZ trpC2*	pTG5951 → PB1078[2]
PB1108	*rsbRA* E148K *rsbRBΔ2 rsbRDΔ2 rsbRCΔ1::ery amyE::ctc-lacZ trpC2*	pTG5974 → PB1078[2]
PB1110	*rsbRA* L149R *rsbRBΔ2 rsbRDΔ2 rsbRCΔ1::ery amyE::ctc-lacZ trpC2*	pTG5978 → PB1078[2]
PB1138	*rsbRA* L146R *rsbRBΔ2 rsbRDΔ2 rsbRCΔ1::ery amyE::ctc-lacZ trpC2*	pTG5976 → PB1078[2]
PB1140	*rsbRA* V139R *rsbRBΔ2 rsbRDΔ2 rsbRCΔ1::ery amyE::ctc-lacZ trpC2*	pTG5977 → PB1078[2]
PB1141	*rsbRA* E136K *rsbRBΔ2 rsbRDΔ2 rsbRCΔ1::ery amyE::ctc-lacZ trpC2*	(3)
PB1147	*rsbRA* K143A *rsbRBΔ2 rsbRDΔ2 rsbRCΔ1::ery amyE::ctc-lacZ trpC2*	pTG6004 → PB1078[2]
PB1148	*rsbRA* E148A *rsbRBΔ2 rsbRDΔ2 rsbRCΔ1::ery amyE::ctc-lacZ trpC2*	pTG6005 → PB1078[2]
PB1149	*rsbRA* L149A *rsbRBΔ2 rsbRDΔ2 rsbRCΔ1::ery amyE::ctc-lacZ trpC2*	pTG6006 → PB1078[2]
PB1151	*rsbRA* Q142A *rsbS* S59A *rsbRBΔ2 rsbRDΔ2 rsbRCΔ1::ery amyE::ctc-lacZ trpC2*	pTG6009 → PB1107[2]
PB1152	*rsbRA* E148K *rsbS* S59A *rsbRBΔ2 rsbRDΔ2 rsbRCΔ1::ery amyE::ctc-lacZ trpC2*	pTG6009 → PB1108[2]
PB1153	*rsbRA* L146A *rsbRBΔ2 rsbRDΔ2 rsbRCΔ1::ery amyE::ctc-lacZ trpC2*	pTG6017 → PB1078[2]
PB1154	*rsbRA* V139A *rsbRBΔ2 rsbRDΔ2 rsbRCΔ1::ery amyE::ctc-lacZ trpC2*	pTG6016 → PB1078[2]
PB1161	*rsbS* S59A *rsbRBΔ2 rsbRDΔ2 rsbRCΔ1::ery amyE::ctc-lacZ trpC2*	(3)
PB1166	*rsbRA* L149D *rsbRBΔ2 rsbRDΔ2 rsbRCΔ1::ery amyE::ctc-lacZ trpC2*	pTG6020 → PB1078[2]
PB1179	*rsbRA* K137A *rsbRBΔ2 rsbRDΔ2 rsbRCΔ1::ery amyE::ctc-lacZ trpC2*	pTG6021 → PB1078[2]
PB1180	*rsbRA* T138A *rsbRBΔ2 rsbRDΔ2 rsbRCΔ1::ery amyE::ctc-lacZ trpC2*	pTG6022 → PB1078[2]
PB1182	*rsbRA* Q142A *amyE::ctc-lacZ trpC2*	pTG5951 → PB198[2]
PB1183	*rsbRA* E148K *amyE::ctc-lacZ trpC2*	pTG5974 → PB198[2]
PB1188	*rsbRA* S140A *rsbRBΔ2 rsbRDΔ2 rsbRCΔ1::ery amyE::ctc-lacZ trpC2*	pTG6023 → PB1078[2]
PB1189	*rsbRA* L141A *rsbRBΔ2 rsbRDΔ2 rsbRCΔ1::ery amyE::ctc-lacZ trpC2*	pTG6024 → PB1078[2]
PB1192	*rsbRA* I144A *rsbRBΔ2 rsbRDΔ2 rsbRCΔ1::ery amyE::ctc-lacZ trpC2*	pTG6025 → PB1078[2]
PB1193	*rsbRA* Q147A *rsbRBΔ2 rsbRDΔ2 rsbRCΔ1::ery amyE::ctc-lacZ trpC2*	pTG6026 → PB1078[2]

[1]Arrow indicates transformation from donor to recipient

[2]Two-step allele replacement

Table S2. Plasmids used for strain construction

Plasmid	Alteration or relevant feature	Reference
pSS4332	Expresses I-*Sce*I for two-step allele replacement	(2)
pTG5916	pUS19-based integrative plasmid. *Nde*I site converted to I-*Sce*I	(3)
pTG5923	*rsbRA* in pTG5916	(3)
pTG5951	*rsbRA* Q142A in pTG5916 (CAA → GCA)	This study
pTG5973	*rsbRA* K143E in pTG5916 (AAA → GAA)	This study
pTG5974	*rsbRA* E148K in pTG5916 (GAG → AAG)	This study
pTG5976	*rsbRA* L146R in pTG5916 (CTG → CGA)	This study
pTG5977	*rsbRA* V139R in pTG5916 (GTA → CGA)	This study
pTG5978	*rsbRA* L149R in pTG5916 (CTG → CGA)	This study
pTG6004	*rsbRA* K143A in pTG5916 (AAA → GCA)	This study
pTG6005	*rsbRA* E148A in pTG5916 (GAG → GCG)	This study
pTG6006	*rsbRA* L149A in pTG5916 (CTG → GCG)	This study
pTG6009	*rsbS* S59A in pTG5916 (TCA → GCA)	(3)
pTG6016	*rsbRA* V139A in pTG5916 (GTA → GCA)	This study
pTG6017	*rsbRA* L146A in pTG5916 (CTG→ GCG)	This study
pTG6020	*rsbRA* L149D in pTG5916 (CTG → GAC)	This study
pTG6021	*rsbRA* K137A in pTG5916 (AAA → GCA)	This study
pTG6022	*rsbRA* T138A in pTG5916 (ACA → GCA)	This study
pTG6023	*rsbRA* S140A in pTG5916 (TCC → GCC)	This study
pTG6024	*rsbRA* L141A in pTG5916 (CTG → GCG)	This study
pTG6025	*rsbRA* I144A in pTG5916 (ATC → GCC)	This study
pTG6026	*rsbRA* Q147A in pTG5916 (CAA → GCA)	This study

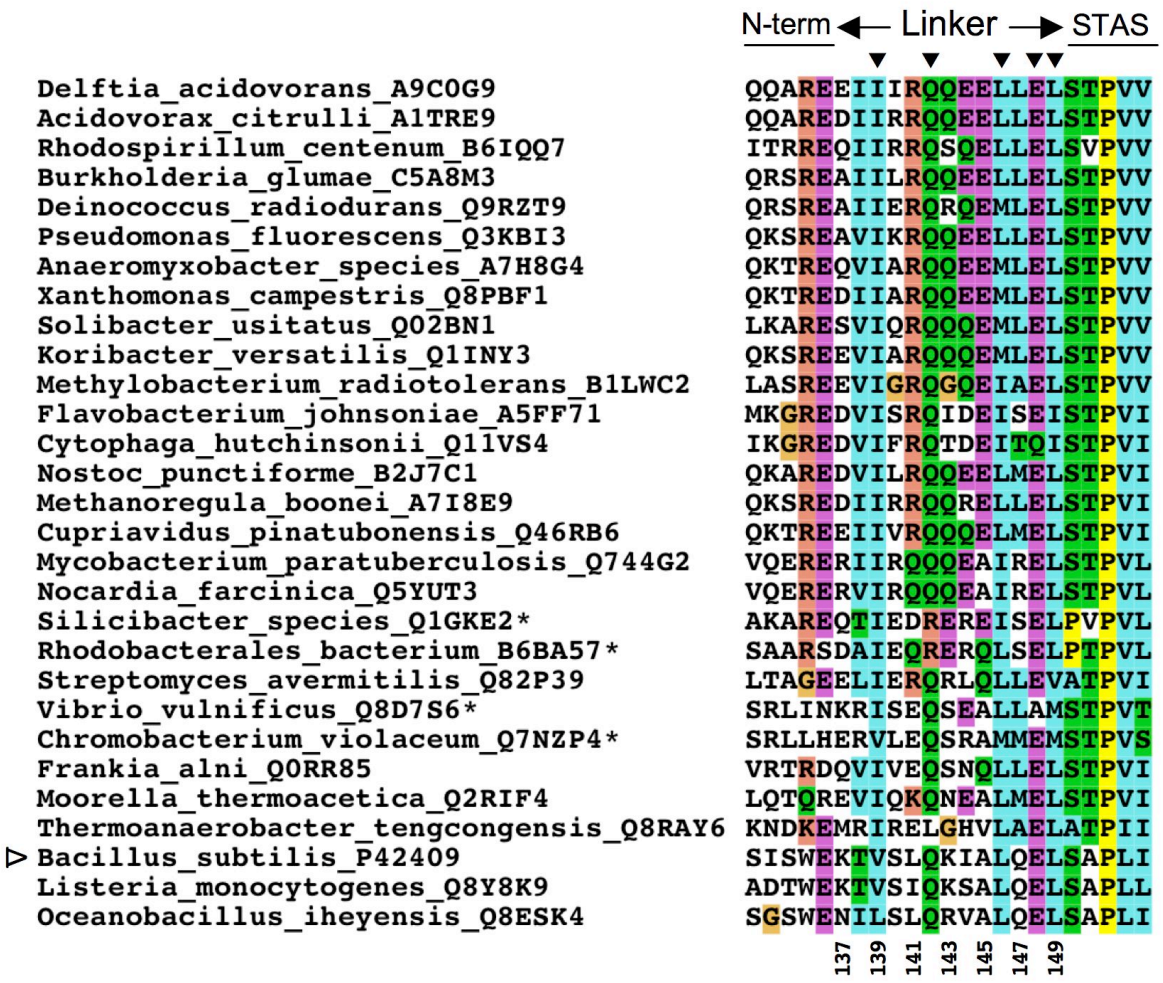

Fig. S1. Clustal W alignment of 29 linker regions from RST modules encoded by diverse microbial genomes. Sequence of each RsbRA homologue is labeled by genus_species and UniProt identifier; these represent one archaeal and seven bacterial phyla. According to the Conserved Domain Database (4), all listed homologues have N-terminal non-heme globin domains except the four protobacterial examples marked by the asterisk following their UniProt indentifier; these four possess heme-binding globin domains. Labels above the alignment indicate five residues from the N-terminal globin domain, the 13-residue linker, and five residues from the C-terminal STAS (sulfate transporter and anti-sigma factor antagonist) domain; filled inverted triangles show five highly conserved linker positions. Numbers beneath the alignment designate residue number within *B. subtilis* RsbRA, whose sequence is marked by the open triangle on the left. Color scheme is standard Clustal W: blue for WLVIMFAC; green for TSNQ; magenta for DE; red for KR, orange for G; and yellow for P.

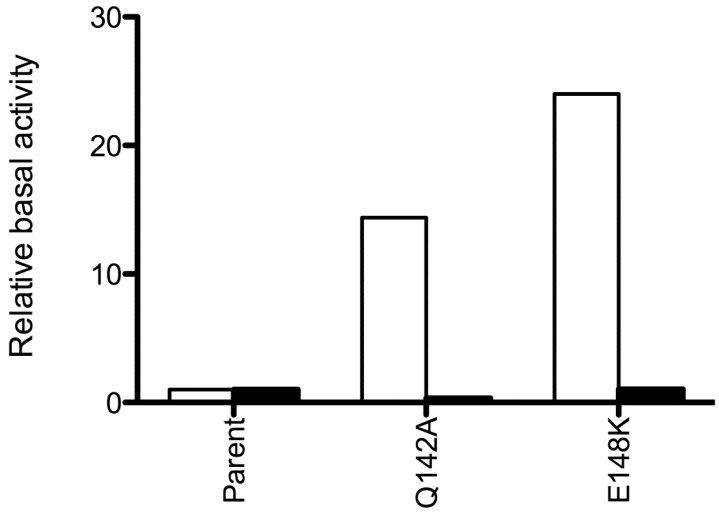

Fig. S2. Presence of all four RsbR co-antogonist paralogs masks the enhancing phenotype caused by linker substitutions in RsbRA. White bars show relative basal level in strains encoding only RsbRA, with data taken from Figure 3; black bars show relative basal activity in strains encoding a full co-antagonist complement: RsbRA, RB, RC and RD. Parent indicates wild type RsbRA, whereas Q142A and E148K indicate RsbRA substitution.

References

1. **Boylan, S. A., A. Rutherford, S. M. Thomas, and C. W. Price.** 1992. Activation of *Bacillus subtilis* transcription factor σ^B by a regulatory pathway responsive to stationary-phase signals. J Bacteriol **174:**3695-706.

2. **Cybulski, R. J., Jr., P. Sanz, F. Alem, S. Stibitz, R. L. Bull, and A. D. O'Brien.** 2009. Four superoxide dismutases contribute to *Bacillus anthracis* virulence and provide spores with redundant protection from oxidative stress. Infect Immun **77:**274-85.

3. **Gaidenko, T. A., X. Bie, E. P. Baldwin, and C. W. Price.** 2011. Substitutions in the presumed sensing domain of the *Bacillus subtilis* stressosome affect its basal output but not response to environmental signals. J Bacteriol **193:**3588-97.

4. **Marchler-Bauer, A., et al.** 2009. CDD: specific functional annotation with the Conserved Domain Database. Nucleic Acids Res **37:**D205-10.